

# Interaction of metal nanoparticles with recombinant arginine kinase from *Trypanosoma brucei*: Thermodynamic and spectrofluorimetric evaluation

O.S. Adeyemi, C.G. Whiteley\*

Department of Biochemistry, Microbiology & Biotechnology, Rhodes University, Grahamstown, South Africa

## ARTICLE INFO

### Article history:

Received 24 July 2013

Received in revised form 21 September 2013

Accepted 25 October 2013

Available online xxxx

### Keywords:

Metal nanoparticle

Thermodynamic fluorimetric analysis

Trypanosomiasis

Arginine kinase

## ABSTRACT

**Background:** *Trypanosoma brucei*, responsible for African sleeping sickness, is a lethal parasite against which there is need for new drug protocols. It is therefore relevant to attack possible biomedical targets with specific preparations and since arginine kinase does not occur in humans but is present in the parasite it becomes a suitable target.

**Methods:** Fluorescence quenching, thermodynamic analysis and FRET have shown that arginine kinase from *T. brucei* interacted with silver or gold nanoparticles.

**Results:** The enzyme only had one binding site. At 25 °C the dissociation ( $K_d$ ) and Stern–Volmer constants ( $K_{sv}$ ) were 15.2 nM, 0.058 nM<sup>-1</sup> [Ag]; and 43.5 nM, 0.052 nM<sup>-1</sup> [Au] and these decreased to 11.2 nM, 0.041 nM<sup>-1</sup> [Ag]; and 24.2 nM, 0.039 nM<sup>-1</sup> [Au] at 30 °C illustrating static quenching and the formation of a non-fluorescent fluorophore–nanoparticle complex. Silver nanoparticles bound to arginine kinase with greater affinity, enhanced fluorescence quenching and easier access to tryptophan molecules than gold. Negative  $\Delta H$  and  $\Delta G$  values implied that the interaction of both Ag and Au nanoparticles with arginine kinase was spontaneous with electrostatic forces. FRET confirmed that the nanoparticles were bound 2.11 nm [Ag] and 2.26 nm [Au] from a single surface tryptophan residue.

**Conclusions:** The nanoparticles bind close to the arginine substrate through a cysteine residue that controls the electrophilic and nucleophilic characters of the substrate arginine–guanidinium group crucial for enzymatic phosphoryl transfer between ADP and ATP.

**General significance:** The nanoparticles of silver and gold interact with arginine kinase from *T. brucei* and may prove to have far reaching consequences in clinical trials.

© 2013 Published by Elsevier B.V.

## 1. Introduction

Among the biomedical target molecules which have been identified as possible drug targets in African sleeping sickness (trypanosomiasis) is arginine kinase (AK), a phosphotransferase enzyme responsible for the reversible formation of phosphoarginine using L-arginine and ATP as substrates [Fig. 1] [1]. Phosphoarginine can act as an emergency reservoir, not only of ATP but also for inorganic phosphate [2–5].

The African disease is caused by the parasite *Trypanosoma brucei* while an equivalent malady in Latin America – Chagas disease – is caused by *Trypanosoma cruzi* [6–8] and both are fatal unless treated. Unfortunately current treatments have limited efficacy, unwanted toxicity,

an emergence of resistant strains of trypanosomes, unsuccessful efforts at vaccine development and the absence of effective anti-trypanosomal therapies coupled with antigenic variation. Consequently there is an ongoing urgent requirement for innovative strategies and the development of new drugs to combat the diseases.

The enzyme AK is absent in humans [9], a fact that makes it the attractive target choice for trypanocide development. Furthermore there is an increased activity of AK in trypanosomes when linked to oxidative stress and since the trypanosomes are being constantly exposed to the pro-oxidants in the blood of mammalian host during their life-cycle the decrease in AK activity would present serious consequences to the growth and survival of the parasites. In light of this, compounds that selectively inhibit AK are desirable and should become candidates for early development of trypanocides.

The nanoscale size of metal nanoparticles allows their unique and remarkable properties to be exploited within the nanomedical fraternity and from our own laboratories have resolved several medical challenges in both infectious (malaria) [10,11] and neurodegenerative

\* Corresponding author at: Department of Biochemistry, Microbiology and Biotechnology, Rhodes University, P.O. Box 94, Grahamstown 6140, South Africa. Tel.: +27 46 6038085; fax: +27 46 6223984.

E-mail address: [C.Whiteley@ru.ac.za](mailto:C.Whiteley@ru.ac.za) (C.G. Whiteley).

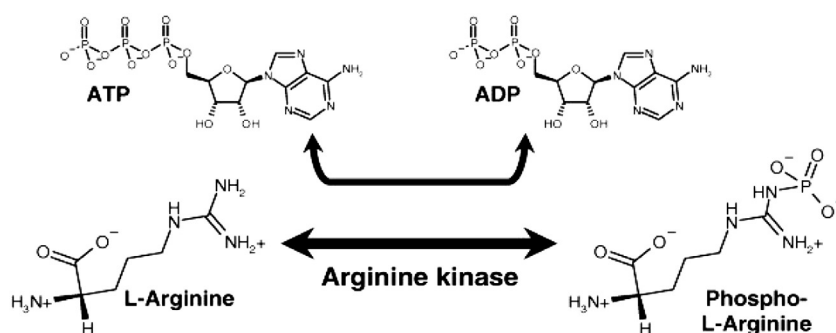


Fig. 1. Enzymatic reaction for arginine kinase.

Q3 diseases (Alzheimer) [12–14]. The present study investigates, from  
75 thermodynamic and spectrofluorimetric points of view the interaction  
76 of silver and/or gold nanoparticles with a recombinant form of AK  
77 enzyme obtained from *T. brucei* (TbAK).

## 78 2. Materials and methods

### 79 2.1. Materials

80 Genomic DNA of *T. brucei* (T927) was a gift from Professor Ullman,  
81 Department of Biochemistry & Biophysics, Oregon Health & Science  
82 University, Portland, Oregon, USA. Enzymes and PCR reagents were  
83 provided by Thermo Fischer Scientific, USA. A Bioflux kit was obtained  
84 from Separation Scientific (South Africa). Oligonucleotides and primers  
85 were from the Integrated DNA Technology (IDT), USA. The clone JET PCR  
86 kit, pSMART and pET-28b (+) as well as the BL21 DE3 and JM 109  
87 strains of *Escherichia coli* were obtained from Fermentas Life Sciences  
Q4 (USA). Absorbance spectroscopy was performed with a Synergy Mx  
89 Monochromator Multi-Mode Microplate Reader (Biotek Instruments,  
90 Inc., USA). All reagents were of analytical grade and obtained from  
Q5 domestic suppliers unless otherwise stated.

### 92 2.2. Assay for TbAK [15]

93 Enzyme extract (20  $\mu$ l) was incubated (5 min, 30  $^{\circ}$ C) with L-arginine  
94 (10 mM), ATP (5 mM), mercaptoethanol (10 mM), and  $MgSO_4$   
95 (200 mM) in Tris-HCl buffer (100 mM, pH 8.6) in a final volume of  
96 170  $\mu$ l. Trichloroacetic acid (180  $\mu$ l, 2.5%) was then added and the  
Q6 whole mixture was heated (100  $^{\circ}$ C, 2 min) to stop the reaction. After  
98 cooling the mixture was treated with ascorbic acid/ammonium molyb-  
99 date (9%, 100  $\mu$ l), left for colour development (5 min), and the absor-  
100 bance was read at 700 nm. The amount of phosphate released was  
101 measured by means of a standard curve as one unit of TbAK activity is  
102 the amount of enzyme that catalyses the formation of 1  $\mu$ mol inorganic  
103 phosphate per minute per ml.

### 104 2.3. Cloning, expression, purification of TbAK [15]

105 Primers of TbAK used to amplify the open reading frame of the TbAK  
106 gene were CAT ATG GGC TTC GGA TCA TCA AAA CCC; (forward; NdeI  
107 restriction site underlined) and CTC GAG CTG TTC CAC GTA CCT  
108 GC; (reverse; XhoI restriction site underlined). The PCR reaction was car-  
Q7 ried out with amplification conditions as follows: Initial denaturation  
110 (98  $^{\circ}$ C, 3 min), 40 cycles of denaturation (98  $^{\circ}$ C, 30 sec), annealing  
111 (62  $^{\circ}$ C, 30 sec; 72  $^{\circ}$ C, 10 sec), and elongation (72  $^{\circ}$ C, 60 sec) in a Biorad  
112 T100 thermal cycler. The 1000 bp product was excised, gel purified  
113 using a Bioflux kit then phosphorylated and blunt ligated into a pSMART  
114 vector using a T4 DNA ligase and finally transformed into JM 109 cells.  
115 The plasmid that contained the TbAK was gel purified using the Bioflux  
116 kit, sequenced and showed 100% identity with the *T. brucei* expressed

product (Accession number – XP\_826998.1) and a high identity with 117  
118 other related guanidino kinases. The plasmid was double digested and a  
119 fragment between NdeI and XhoI restriction sites containing the TbAK  
120 gene was excised from the plasmid and subcloned into a pET-28b (+) ex-  
121 pression vector previously treated with NdeI and XhoI. This plasmid tran-  
122 scribes under the control of the T7 promoter and includes a polyhistidine  
123 tag. This was transformed into BL21 DE3 cells, grown overnight, at 37  $^{\circ}$ C,  
124 in 50 ml LB culture medium containing kanamycin after which an aliquot  
125 (5.0 ml) was transferred into a 2 l flask containing auto-media culture  
126 (500 ml). This was grown (20  $^{\circ}$ C, 150 rpm, 36 h) and the cells harvested  
127 (6000  $\times$ g, 10 min), washed twice with Tris buffered saline (Tris-HCl,  
128 50 mM; NaCl, 150 mM; pH 7.5) and lysed (freeze-thawed [–80  $^{\circ}$ C/  
129 4  $^{\circ}$ C; 2 cycles]) in lysis buffer [NaH<sub>2</sub>PO<sub>4</sub> buffer (50 mM, pH 7.6) contain-  
130 ing NaCl (300 mM), glycerol (10%), Tween (0.25%), imidazole (10 mM),  
131 mercaptoethanol (10 mM), phenylmethylsulphonylfluoride (1 mM)].  
132 The lysed cells were centrifuged (2700  $\times$ g, 30 min) and the supernatant  
133 was centrifuged (100,000  $\times$ g, 90 min) after which the supernatant  
134 (150 ml) was loaded onto a Ni-nitrilotriacetic acid affinity column previ-  
135 ously washed with the same lysis buffer. The fusion protein was eluted  
136 with increasing amounts of imidazole (0–500 mM) in Hepes buffer  
137 (10 mM, pH 7.5) and concentrated using vivaspin (GE Healthcare,  
138 Sweden) and then purified by FPLC on a Superdex 200 HR 10/30 column  
139 with Hepes buffer (25 mM, pH 7.6) containing glycerol (15%), EDTA  
140 (0.1 M), KCl (1 M) at a flow rate of 1 ml  $\cdot$ min<sup>–1</sup>. Proteins were resolved  
Q8 by SDS-PAGE in order to confirm purity of fractions before pooling. All  
141 purification procedures were carried out at 4  $^{\circ}$ C.

### 142 2.4. Characterisation of TbAK

143 The purity of TbAK was assessed by SDS-PAGE analysis and its opti-  
144 mum temperature, thermal stability, pH optimum and kinetic paramet-  
145 ers ( $K_m$  and  $V_{max}$ ) were established [15].  
146

### 147 2.5. Synthesis and characterization of gold and silver nanoparticles

148 Gold and silver nanoparticles were synthesised, respectively, from ei-  
149 ther AuCl<sub>3</sub> or AgNO<sub>3</sub> and stabilized with tannic acid/polyvinylpyrrolidone.  
150 The pale yellow solution (Ag-NPs) and the wine red solution (Au-NPs)  
151 were filtered using the 0.22  $\mu$ m filter and characterised by UV/Vis  
152 spectrophotometry, inductively coupled plasma optical emission spec-  
153 trometry (ICP-OES), energy dispersive X-ray spectroscopy (EDX) and  
154 transmission electron microscopy (TEM) [15].  
Q9

### 155 2.6. Fluorimetric analysis of the interaction of nanoparticles with TbAK

156 Structural changes induced in TbAK by the interaction of the silver/  
157 gold nanoparticles were determined spectrofluorimetrically at an excita-  
158 tion wavelength of 295 nm, the wavelength at which tryptophan  
159 absorbs, and an emission wavelength of 350 nm. The change in fluores-  
160 cence of a solution was monitored at 25  $^{\circ}$ C, over 10 min, as increasing

161 concentrations of the respective nanoparticles (0–50 nM) were added to  
 162 a reaction mixture of TbAK (5 μl) in triethanolamine buffer (pH 7.4,  
 163 10 mM) containing NaCl (100 mM) in a final volume of 200 μl. All  
 164 fluorescence quenching experiments were performed at 25 °C [298 K]  
 165 and 30 °C [303 K].

166 2.7. Statistical analyses

167 All analyses were carried out in triplicate and values were reported  
 168 as the means with standard deviation  $p < 0.05$  versus controls. Analysis  
 169 of variance was conducted using Statistica for Windows, version 8  
 170 (Statsoft Inc.) and Microsoft Excel 2010.

171 3. Results and discussion

172 3.1. Binding site for nanoparticles on TbAK

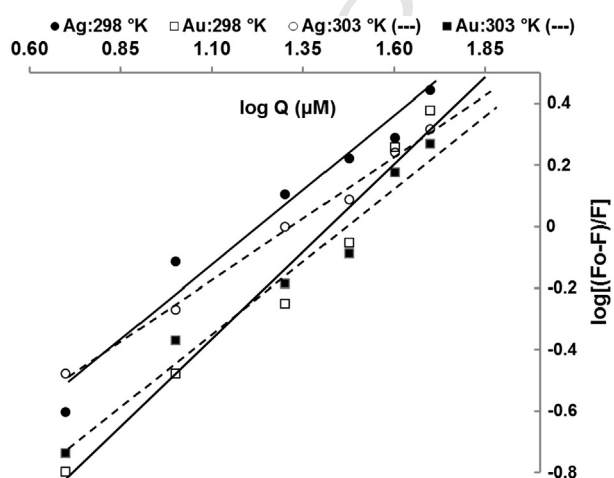
173 The binding parameters of nanoparticles for TbAK can be analysed  
 174 accordingly [Eq. (1)].  
 175

$$\text{Log}[(F_0 - F)/F] = \text{log}K_a + n \text{log}[Q] \quad (1)$$

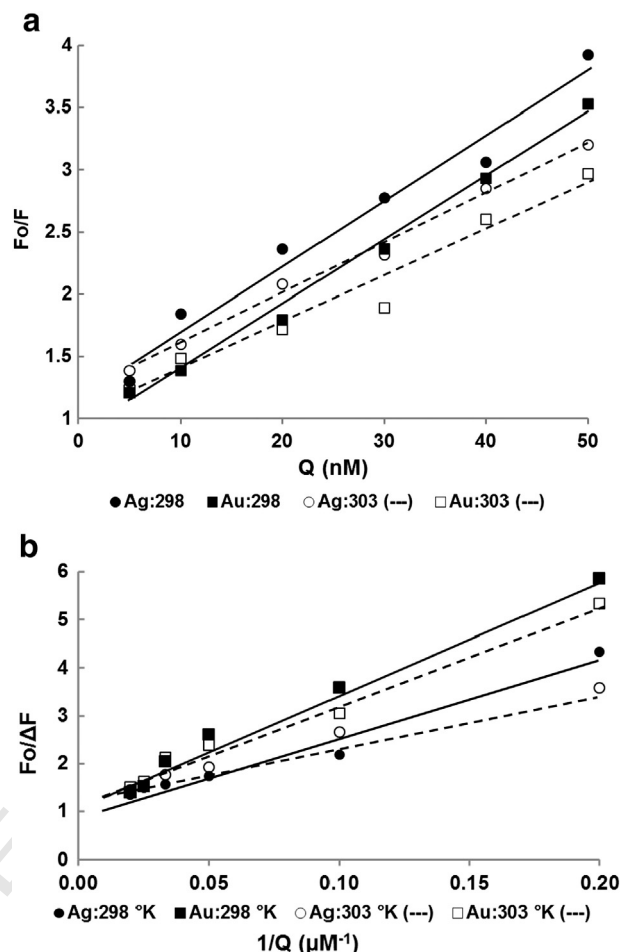
176 where  $F_0$  and  $F$  are the fluorescent intensities of TbAK in the absence and  
 177 presence of either silver or gold nanoparticles respectively;  $Q$  is the con-  
 178 centration of nanoparticles; 'n' is the number of binding sites (on the pu-  
 179 rified enzyme available for the particles), and  $K_a$  is the association  
 180 constant [and its reciprocal dissociation constant ( $K_d$ )]. Both 'n' and  $K_a$   
 181 were estimated, respectively, from the slope of the linear regressions  
 182 and the intercept on the  $\text{log} [(F_0 - F) / F]$  axis [Fig. 2] [16]. For both  
 183 Ag and Au nanoparticles only 1 binding site was available. The values  
 184 obtained for the binding constants ( $K_d$ ) [15.2 nM for Ag; 43.5nM for Au  
 185 nanoparticles] indicated a strong affinity between TbAK and the nanopar-  
 186 ticles. As the temperature increased from 25 °C [298 K] to 30 °C [303 K]  
 187 these  $K_d$  values changed slightly to 11.12 nM (Ag); 24.21 nM (Au).  
 188

189 3.2. Fluorescence quenching analysis

190 The binding of the nanoparticles caused a quenching in the trypto-  
 191 phan fluorescence of TbAK [Fig. 3a; b] with linearity in the Stern–Volmer  
 192 plots implying that one, or more, tryptophan residues are close to the  
 193 binding site. The possible quenching mechanism can be interpreted  
 194 from the fluorescence analysis data and analysed according to the



195 **Fig. 2.** Hill plots of  $\text{log} [(F_0 - F)/F]$  versus  $\text{log} [Q]$  for the binding of Ag and Au nano-  
 196 particles (0–50 nM) with TbAK (5 μl) in triethanolamine buffer (pH 7.4, 10 mM)  
 197 containing NaCl (100 mM) in a final volume (200 μl) at two different temperatures  
 198 (●), [Ag – 298 K], (● –), [Ag – 303 K]; (■), [Au – 298 K], (■ –), [Au – 303 K].  
 199  $\lambda_{\text{ex}} = 295$  nm and  $\lambda_{\text{em}} = 350$  nm.



200 **Fig. 3.** a: Stern–Volmer plots for fluorescence quenching for the binding of Ag and Au  
 201 nanoparticles (0–50 nM) with TbAK (5 μl) in triethanolamine buffer (pH 7.4, 10 mM)  
 202 containing NaCl (100 mM) in a final volume (200 μl) at two different temperatures (●),  
 203 [Ag – 298 K], (● –), [Ag – 303 K]; (■), [Au – 298 K], (■ –), [Au – 303 K].  
 204  $\lambda_{\text{ex}} = 295$  nm and  $\lambda_{\text{em}} = 350$  nm. b: Double reciprocal plots (modified Stern–Volmer)  
 205 for the binding of Ag and Au nanoparticles (0–50 nM) with TbAK (5 μl) in triethanolamine  
 206 buffer (pH 7.4, 10 mM) containing NaCl (100 mM) in a final volume (200 μl) at two dif-  
 207 ferent temperatures (●), [Ag – 298 K], (● –), [Ag – 303 K]; (■), [Au – 298 K], (■ –),  
 208 [Au – 303 K].  $\lambda_{\text{ex}} = 295$  nm and  $\lambda_{\text{em}} = 350$  nm.

209 Stern–Volmer equations [Eqs. (2), (3)]. The Stern–Volmer constant  
 210 ( $K_{SV}$ ) was estimated from the slope of the linear regression and  $\theta$ , the  
 211 fraction of tryptophan residues near the surface of the enzyme, from  
 212 the reciprocal of the y-intercept [Fig. 3b].

$$F_0/\Delta F = 1/(\theta K_{SV}Q) + 1/\theta \quad (2)$$

$$F_0/F = 1 + K_{SV}Q \quad (3)$$

204 where  $\Delta F = F_0 - F$ . The 'y intercept' from the Stern–Volmer plots  
 205 [Fig. 3a] was equivalent to 1, thereby indicating that fluorescence was  
 206 only due to internal quenching by the nanoparticle and not the interplay  
 207 of other fluors in solution which may result in external quenching. Res-  
 208 pective  $K_{SV}$  values for Ag- and Au-nanoparticles were  $0.058 \text{ nM}^{-1}$   
 209 and  $0.052 \text{ nM}^{-1}$ . As the temperature changed from 25 °C [298 K] to  
 210 30 °C [303 K] the respective  $K_{SV}$  values decreased to  $0.041 \text{ nM}^{-1}$  and  
 211  $0.039 \text{ nM}^{-1}$  [Fig. 3a] illustrating that the quenching by the nanopar-  
 212 ticles must be classified as static supported by the formation of a non-  
 213 fluorescent fluorophore–nanoparticle complex [17,18].

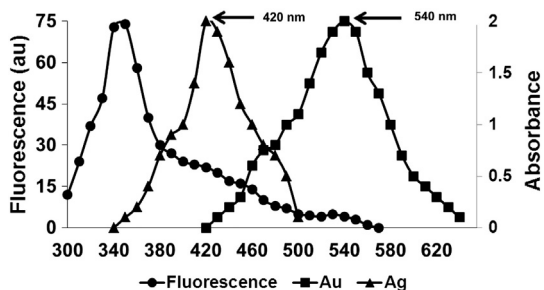


Fig. 4. Spectral overlap of fluorescence emission spectrum of TbAK and absorbance spectra for Au and Ag nanoparticles with plasmon resonance maxima indicated at 420 nm and 540 nm.

### 3.3. Fluorescence energy transfer (FRET)

Fluorescence quenching of Trp within the TbAK active site can also be used by a process of energy transfer (FRET) that allows for the measurement of the relative distance ( $r$ ) between this tryptophan and the bound nanoparticle according to Förster's theory [19]. Since there is spectral overlap of the fluorescence emission spectrum of TbAK and the UV absorption spectra of the Ag and Au nanoparticles [Fig. 4] this distance ( $r$ ) can be calculated from the efficiency of energy transfer ( $E$ ) [Eq. (4)].

$$E = 1 - F/F_0 = R_0^6 / (R_0^6 + r^6) \quad (4)$$

$$R_0^6 = 8.79 \times 10^{-25} \kappa^2 \eta^{-4} \phi \left[ \sum \int F_\lambda \cdot \varepsilon_\lambda \cdot \lambda^4 \cdot \Delta\lambda \right] / \left[ \sum \int F_\lambda \cdot \Delta\lambda \right] \quad (5)$$

where  $R_0$  = Förster distance when efficiency of transfer is 50% and depends on the relative orientation of the tryptophan and nanoparticle ( $\kappa$ ), the refractive index of the medium ( $\eta$ ), the quantum fluorescence yield ( $\phi$ ),  $F_\lambda$  is the fluorescence intensity of the tryptophan at wavelength ( $\lambda$ ) and  $\varepsilon_\lambda$  is the molar absorption coefficient of the nanoparticle at

wavelength ( $\lambda$ ); the integral overlap of the fluorescence emission spectrum of TbAK and the absorption spectrum of the Ag nanoparticle is represented within the integration symbols [Eq. (5)].

Assuming  $\kappa^2 = 0.667$ ;  $\phi = 0.118$ ; and  $\eta = 1.336$  [12,20] then from Eqs. (4) and (5),  $R_0$  and  $r$  for Ag and Au nanoparticles are estimated as 2.18, 2.11 nm and 2.35, 2.26 nm respectively. According to literature, any value for this distance ( $r$ ) that is less than 10 nm and falls between 0.5 and 1.5 of the  $R_0$  value indicates a high probability that fluorescence transfer is taking place [21].

An in-depth molecular modelling and docking study of the interaction and binding of these nanoparticles to TbAK is currently on going and will be reported elsewhere. As far as we were aware no crystallographic structure for arginine kinase from *T. brucei* had been deposited in the Protein Data Bank. On the other hand that for *T. cruzi* [TcAK] had been reported [22] with 82% analogy [23] to *T. brucei*. The analysis of the primary structure of TcAK [PDB ID: 2J1Q] reveals only 2 tryptophan residues – one buried near the ATP/ADP active binding site [Trp<sup>221</sup>] and one on the surface of the enzyme [Trp<sup>104</sup>] [24]. FRET studies confirmed that the nanoparticles quenched the fluorescence of only one tryptophan residue, most probably the surface Trp<sup>104</sup>, as  $\theta$  [Eq. (2)] [Fig. 3b] was equal to 1 for both types of nanoparticles and at both temperatures.

The interatomic distance between NH<sub>1</sub> of the arginine substrate and the aromatic ring of Trp<sup>104</sup> is 22.2 Å (2.22 nm) [Fig. 5] while that for Trp<sup>221</sup> is 15.1 Å (1.51 nm). Furthermore a thiolate sulphur atom from Cys<sup>271</sup> is only 3.3 Å from this reactive N<sub>1</sub>. The present findings from FRET analysis indicate that the distances between Trp<sup>104</sup> and the bound nanoparticles are 2.11 nm and 2.26 nm for Ag and Au respectively.

It is well known from our other studies on apoferritin/ferroxidase, GroEL/ATPase and comparative study with human/*Plasmodium falciparum* superoxide dismutase (hSOD/PfSOD) [10,11,25] that both Ag and Au nanoparticles have not only catalytic properties but a strong affinity to the thiol (SH) group of cysteine residues. From a structural and mechanistic point of view the distance between critical amino acid residues within the active regions of these enzymes was about 2.5–4.0 Å well within the range for the nanoparticles to bind. This affected the nucleophilic character of these amino acids altering

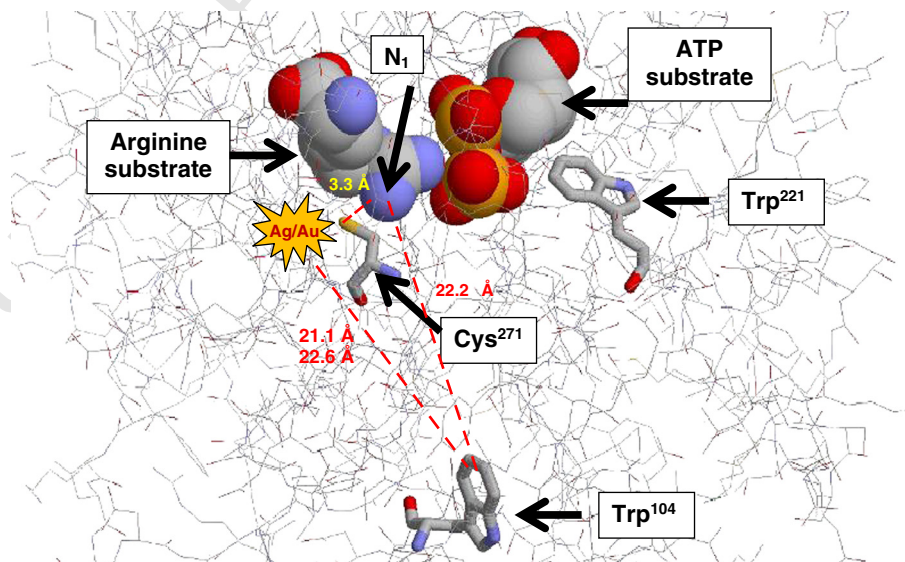


Fig. 5. Proposed structure of the binding sites for TbAK showing the interaction of silver/gold nanoparticles through Cys<sup>271</sup>, interfering with N<sub>1</sub> of the arginine substrate. The interatomic distance between the thiolate atom of Cys<sup>271</sup> and N<sub>1</sub> of the arginine substrate is 3.3 Å. The interatomic distance between Trp<sup>104</sup> and N<sub>1</sub> is 22.2 Å while that distance between Trp<sup>104</sup> and bound Ag/Au nanoparticles is 21.1 Å and 22.6 Å respectively. Nitrate not shown.

the binding of Fe<sup>2+</sup> (ferroxidase) and/or Cu<sup>+</sup> (hSOD) to the nanoparticles and consequently changing the rate of electron removal and oxidation to Fe<sup>3+</sup> and/or Cu<sup>2+</sup>. The interaction of the nanoparticles facilitates the formation of a respective hydrolysis product (FeOOH; H<sub>2</sub>O<sub>2</sub>). In hSOD Cys<sup>57</sup> and Cys<sup>146</sup> are 2.08 Å apart and nanoparticle binding changes the conformation of the reactive core and changes the rate of addition of oxidant. These two amino acids are not present in PfsOD. With respect to ferritin/ferroxidase – three Cys<sup>126</sup> residues from three different chain are juxtaposed within 3.6 Å from the Fe<sup>2+</sup>/Fe<sup>3+</sup> core suggesting that the gold/silver nanoparticles interact at these positions and with exposed-SH groups leading to altered activity.

Consequently, based upon this discussion, it is well within the realm of possibility that the nanoparticles would interact with the sulphur atom of Cys<sup>271</sup> [Fig. 5]. This would decrease its electronegativity and, in turn, decrease the nucleophilicity of the N<sub>1</sub> of the arginine substrate towards attack on the γ-phosphoryl group of ATP. With the enzymatic formation of ATP, a blocking of the thiolate by nanoparticles would prevent its acceptance of a proton from the arginine guanidinium group decreasing the overall phosphoryl transfer to ADP.

### 3.4. Thermodynamic analysis

In order to elucidate the interactive forces between TbAK and Au/Ag nanoparticles temperature-dependent thermodynamic parameters were calculated according to van't Hoff [Eq. (6)]; ΔG was also estimated [Eq. (7)].

$$\ln K_{sv} = -(\Delta H/RT) + (\Delta S/R) \quad (6)$$

$$\Delta G = \Delta H - T\Delta S \quad (7)$$

where R = gas constant (8.314 J mol<sup>-1</sup> K<sup>-1</sup>); ΔH = enthalpy change, ΔS = entropy change, ΔG = free energy change and K<sub>sv</sub> = Stern-Volmer binding constant at the corresponding temperature (T, K). Since the Stern-Volmer plot was linear [Fig. 3a] and the quenching mechanism by the nanoparticles classified as a static one K<sub>sv</sub> can be equated to K<sub>s</sub> [18].

According to enthalpy change (ΔH) and entropy change (ΔS), the model of interaction between any ligand and protein can be concluded as: (1) ΔH > 0 and ΔS > 0 are indicative of hydrophobic forces; (2) ΔH < 0 and ΔS < 0 are indicative of Van de Waals interactions and hydrogen bonds; and (3) ΔH < 0 and ΔS > 0 are indicative of electrostatic interactions [26,27]. Consequently negative ΔH, positive ΔS and negative ΔG values from the interaction of both Ag and Au nanoparticles with TbAK (Table 1) implied that not only were electrostatic forces operative during the binding but also the interaction was spontaneous and governed by large thermodynamically favourable entropies, confirmed by the large positive values of ΔS: 152.74 J mol<sup>-1</sup> K<sup>-1</sup>, (Ag nanoparticles) and 116.59 J mol<sup>-1</sup> K<sup>-1</sup>, (Au nanoparticles).

## 4. Conclusions

A thorough investigation of the interaction of silver and gold nanoparticles with TbAK in terms of thermodynamic and spectrofluorimetric

analyses has been undertaken. Binding constants obtained were consistent with a spontaneous static quenching, governed by large thermodynamically favourable positive entropies, and negative ΔH and ΔG values that supported electrostatic forces in operation. FRET analysis estimated the binding distance between Trp<sup>104</sup> and Ag nanoparticle to be 2.11 nm while that for Au to be 2.26 nm.

## Acknowledgements

This research was supported by the National Research Foundation (NRF) South Africa. We want to thank Prof. Buddy Ullman (Department of Biochemistry & Biophysics, Oregon State University, USA) and Dr. Jacqui van Marwijk (Postdoctoral fellow, Department of Biochemistry, Microbiology & Biotechnology, Rhodes University, Grahamstown, South Africa).

## References

- C.A. Pereira, G.D. Alonso, M.C. Paveto, M.M. Flawiá, H.N. Torres, L-arginine uptake and L-phosphoarginine synthesis in *Trypanosoma cruzi*, J. Eukaryot. Microbiol. 46 (6) (1999) 566–570.
- C.A. Pereira, G.D. Alonso, S. Ivaldi, A. Silver, M.J. Alves, H.N. Torres, M.M. Flawiá, Arginine kinase overexpression improves *Trypanosoma cruzi* survival capability, FEBS Lett. 554 (1–2) (2003) 201–205.
- L.D. Andrews, J. Graham, M.J. Snider, D. Fraga, Characterisation of a novel bacterial arginine kinase from *Desulfotalea psychrophila*, Comp. Biochem. Physiol. B Biochem. Mol. Biol. 150 (3) (2008) 312–319.
- W.R. Ellington, Evolution and physiological roles of phosphagen system, Annu. Rev. Physiol. 63 (2001) 289–325.
- K. Uda, N. Fujimoto, Y. Akiyama, K. Mizuta, K. Tanaka, W.R. Ellington, T. Suzuki, Evolution arginine kinase gene family, Comp. Biochem. Physiol. D Genomics Proteomics 1 (2) (2006) 209–218.
- F. Canonaco, U. Schlattner, P.S. Pruet, T. Wallimann, U. Sauer, Functional expression of arginine kinase improves recovery from pH stress of *Escherichia coli*, Biotechnol. Lett. 25 (13) (2003) 1013–1017.
- F. Canonaco, U. Schlattner, P.S. Pruet, T. Wallimann, U. Sauer, Functional expression of phosphagen kinase systems confers resistance to transient stresses in *Saccharomyces cerevisiae* by buffering the ATP pool, J. Biol. Chem. 277 (35) (2002) 31303–31309.
- C.A. Pereira, L.A. Bouvier, M.M. Cámara, M.R. Miranda, Singular features of Trypanosomatids' phosphotransferases involved in cell energy management, Enzyme Res. (2011), <http://dx.doi.org/10.4061/2011/576483>.
- M.R. Miranda, G.E. Canepa, L.A. Bouvier, C.A. Pereira CA, *Trypanosoma cruzi*: oxidative stress induces arginine kinase expression, Exp. Parasitol. 114 (4) (2006) 341–344.
- A. Sennuga, J. van Marwijk, C.G. Whiteley, Ferritin activity of apoferritin is increased in the presence of platinum nanoparticles, Nanotechnology (2012), <http://dx.doi.org/10.1088/0957-4484/23/3/035102>.
- A. Sennuga, J. van Marwijk, C.G. Whiteley, Multiple fold increase in activity of ferroxidase–apoferritin complex by silver and gold nanoparticles, Nanomed. Nanotechnol. Biol. Med. 9 (2) (2013) 185–193.
- E.R. Padayachee, C.G. Whiteley, Spectrofluorimetric analysis of amyloid peptides with neuronal nitric oxide synthase: implications in Alzheimer's disease, Biochim. Biophys. Acta 1810 (2011) 1136–1140.
- E.R. Padayachee, C.G. Whiteley, Interaction of glycine zipper fragments of Aβ-peptides with neuronal nitric oxide synthase: kinetic, thermodynamic and spectrofluorimetric analysis, Neuropeptides 47 (2013) 171–178.
- E.R. Padayachee, N. Ngqwala, C.G. Whiteley, Association of β-amyloid peptide fragments with neuronal nitric oxide synthase: implications in the etiology of Alzheimers disease, Enzyme Inhib. Med. Chem. 27 (3) (2012) 356–364.
- O.S. Adeyemi, C.G. Whiteley, Interaction of nanoparticles with arginine kinase from *Trypanosoma brucei*: kinetic and mechanistic evaluation, Int. J. Biol. Macromol. (2013)(accepted for publication).
- M.X. Xie, X.Y. Xu, Y.D. Wang, Interaction between hesperetin and human serum albumin revealed by spectroscopic methods, Biochim. Biophys. Acta Gen. Subj. 1724 (1–2) (2005) 215–224.
- A.S. Al-Kady, M. Geber, M.M. Hussein, E.M. Ebeida, Structural and fluorescence quenching characterisation of hematite nanoparticles, Spectrochim. Acta 83 (2011) 398–405.
- D.E. Schlammadinger, D.J. Kats, J.E. Kim, Quenching of tryptophan fluorescence in unfolded cytochrome c: biophysics experiment for physical chemistry students, J. Chem. Educ. 87 (9) (2010) 961–964.
- T. Förster, Intermolecular energy migration and fluorescence, Ann. Phys. 2 (1948) 55–75.
- H. Wang, W. Zhu, X. Wang, Mechanism of inhibition of arginine kinase by flavonoids consistent with thermodynamics of docking simulation, Int. J. Biol. Macromol. 49 (5) (2011) 985–991.
- Y. Chen, J.D. Mills, A. Periasamy, Protein localization in living cells and tissues using FRET and FLIM, Differentiation 71 (2003) 528–554.

**Table 1**  
Thermodynamic parameters estimated for the interaction between arginine kinase of *Trypanosoma brucei* (TbAK) and Ag/Au nanoparticles at two different temperatures.

Nanoparticle	T (K)	ΔH (kJ·mol <sup>-1</sup> )	ΔG (kJ·mol <sup>-1</sup> )	ΔS (J mol <sup>-1</sup> K <sup>-1</sup> )
Ag	298	-52.55	-98.07	152.74
	303		-98.83	
Au	298	-42.08	-76.82	116.59
	303		-77.38	

- 396 [22] P. Fernandez, A. Haouz, C.A. Pereira, C. Aguilar, P.M. Alzari, The crystal structure of 404  
397 *Trypanosoma cruzi* arginine kinase, *Proteins* 69 (2007) 209–214. 405
- 398 [23] C.A. Pereira, G.D. Alonso, H.N. Torres, M.M. Flawiá, Arginine kinase: a common 406  
399 feature for management of energy reserves in African and American flagellat- 407  
400 ed trypanosomatids, *J. Eukaryot. Microbiol.* 49 (1) (2002) 82–85. 408
- 401 [24] X. Wu, W. Zhu, Z. Lü, Y. Xia, J. Yang, F. Zou, X. Wang, The effect of rutin on arginine 409  
402 kinase: inhibition kinetics and thermodynamics merging with docking simulation, 410  
403 *Int. J. Biol. Macromol.* 44 (2) (2009) 149–155. 411
- [25] A. Sennuga, J. van Marwijk, A. Boshoff, C.G. Whiteley, Enhanced activity of 404  
chaperonin GroEL in the presence of platinum nanoparticles, *J. Nanopart. Res.* 14 405  
(5) (2012), <http://dx.doi.org/10.1007/s11051-012-0824-6>. 406
- [26] P.D. Ross, S. Subramanian, Thermodynamics of protein association reactions: forces 407  
contributing to stability, *Biochemistry* 20 (1981) 3096–3102. 408
- [27] S. Strazza, R. Hunter, E. Walker, D.W. Darnall, The thermodynamics of bovine 409  
and porcine insulin determined by concentration difference spectroscopy, 410  
*Arch. Biochem. Biophys.* 238 (1985) 30–42. 411  
412

UNCORRECTED PROOF